2018 24th International Conference on Pattern Recognition (ICPR)
Beijing, China, August 20-24, 2018

Automatically Detecting Arrhythmia-related Irregular Patterns using the Temporal and Spectro-Temporal Textures of ECG Signals

Sara S. Abdeldayem and Thirimachos Bourlai
Lane Department of Computer Science and Electrical Engineering
West Virginia University, Morgantown, WV 26506 USA
ssa0006@mix.wvu.edu, Thirimachos.Bourlai@mail.wvu.edu

***Abstract*—Arrhythmia is an abnormal heart rhythm that occurs due to the improper operation of the electrical impulses that coordinate the heartbeats. It is one of the most well-known heart conditions (including coronary artery disease, heart failure etc.) that is experienced by millions of people around the world. While there are several types of arrhythmias, not all of them are dangerous or harmful. However, there are arrhythmias that can often lead to death in minutes (e.g. ventricular fibrillation and ventricular tachycardia) even in young people. Thus, the detection of arrhythmia is critical for stopping and reversing its progression and for increasing longevity and life quality. While a doctor can perform different heart-monitoring tests specific to arrhythmias, the electrocardiogram (ECG) is one of the most common ones used either independently or in combination with other tests (to only detect, e.g. echocardiogram, or trigger arrhythmia and, then, detect, e.g. stress test). We propose a machine learning approach that augments the traditional arrhythmia detection approaches via our automatic arrhythmia classification system. It utilizes the texture of the ECG signal in both the temporal and spectro-temporal domains to detect and classify four types of heartbeats. The original ECG signal is first preprocessed, and then, the R-peaks associated with heartbeat estimation are identified. Next, 1D local binary patterns (LBP) in the temporal domain are utilized, while 2D LBPs and texture-based features extracted by a grayscale co-occurrence matrix (GLCM) are utilized in the spectro-temporal domain using the short-time Fourier transform (STFT) and Morse wavelets. Finally, different classifiers, as well as different ECG lead configurations are examined before we determine our proposed time-frequency SVM model, which obtains a maximum accuracy of 99.81%, sensitivity of 98.17%, and specificity of 99.98% when using a 10 cross-validation on the MIT-BIH database. Our approach yields competitive accuracy when compared to other methods discussed in the literature.**

I. Introduction

Cardiac arrhythmias pertain to a group of diseases where the heart fails to contract or beat at the correct rhythm. It is considered a common cause of death and affects more than one million individuals in USA alone [1]. While the electrocardiogram (ECG) is one of the most widely used tests used to diagnose different types of cardiac diseases, there are other types of non-implanted heart rhythm monitoring systems. These include the Holter monitor (a wearable device that records a continuous ECG), and the event monitor (similar to Holter but it records for a few minutes only at specific times of each day when someone wears it). Whatever the type of heart rhythm monitoring used, the disorders affecting the electrical activity of the heart due to the presence of specific arrhythmia can be reflected in the patient's ECG recorded pattern. Thus, a doctor can use the ECG signal of a patient to detect heart abnormalities (e.g. a faster or slower than normal, or an irregular heartbeat), and if the doctor finds any abnormality, she/he may propose the usage of additional tests to determine whether a treatment is necessary.

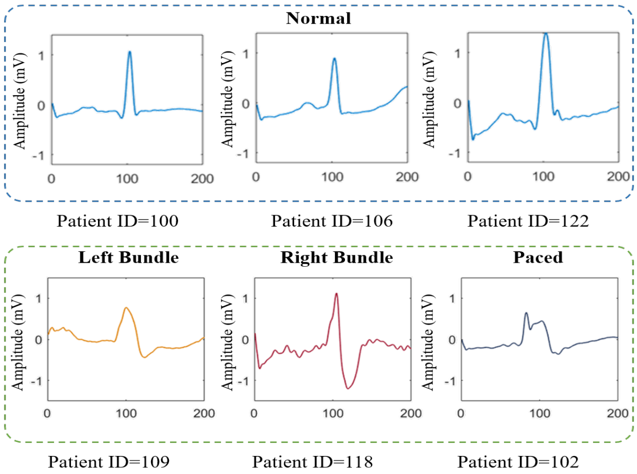

Fig. 1 Different arrhythmia patterns based on the ECG signals of four randomly selected patients, where the x-axis is the data points and y-axis is the signal amplitude in (mV).

While the aforementioned traditional arrhythmia detection approaches used by licensed medical practitioners to perform ECG tests are very important, alternative, computer-based approaches can also be used. These software-based approaches do not require the presence of a medical expert to run. They can be installed in any computer, where a graphical user interface can be used to load an ECG signal of a patient and then, modern signal processing and machine learning algorithms will run that can decide whether the patient has a normal or an abnormal arrhythmia pattern detected. Such a capability, namely a computer-aided design to automatically detect and classify cardiac events by a single computer, can be beneficial to the hands of either a doctor who may need to assess multiple ECG signals from many patients in a timely manner, or a system operator that may detect an abnormality in an ECG signal and, then, contact a doctor to verify the findings and move forward with a potential treatment. Thus, it reduces

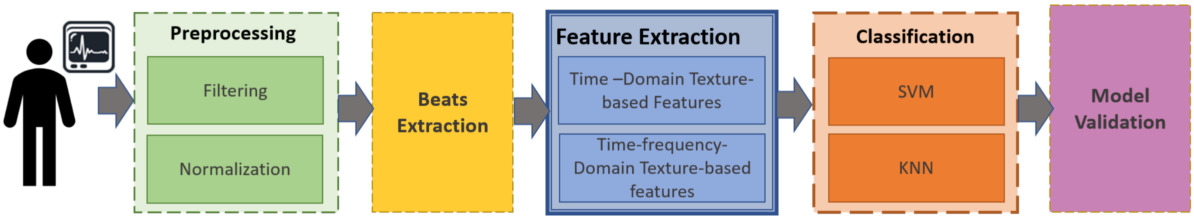

Fig. 2 Workflow of the proposed approach.

the error that might be resulted from subjective diagnosis, and can be used in rural areas where professional physician may not be available.

There are several computer-aided approaches in the literature that extract a set of features from an original ECG signal to detect arrhythmia [2]. Nevertheless, there are different challenges that impact the efficiency of the proposed algorithmic modules used for arrhythmia detection due to a number of factors. These include the time-varying nature of the ECG signal, each patient's physiological condition during the ECG recording, as well as each patient's physiological condition overall, which depends on their age, gender, current or recent medication and/or medical history.

The computer-aided arrhythmia detection approaches can be categorized into three main groups based on the type of features used for processing by the classification algorithm, namely time-domain, frequency-domain, and time-frequency domain features. The time-domain features employ the amplitude of the ECG signal that changes with time. For example, Mazhar et al. [3] first extracted the QRS fiducial points from the signal, and then to used statistical features, such as mean, standard deviation, and energy for classification. Dewangan, and Shukla [4] detected the P-R-T fiducial points using a windowing technique. Then, morphological features were extracted including the R peak amplitude, PR interval, and the wavelet transform coefficients to feed a neural network classifier. In addition, Yu SN, and Chou KT [5] proposed a method to classify ECG signals using independent component analysis (ICA) coefficients and RR intervals as features, and a neural network as a classifier. Pan at el. [6] used a Hidden Markov Model (HMM) to classify three different types of heartbeats, such as bundle branch block, ventricular premature contraction, and atrial premature contraction using MIT-BIH database. They compared the performance of their HMM-based classifier to other ones (such as neural networks, and restricted coulomb energy networks). Although their proposed approach outperformed other methodologies, they combined both the left and right block bundle into one group.

Nonetheless, some of the research approached study the usage of frequency domain based features that can also be used for arrhythmia detection. For example, Desai at el. [7] propose such a method that first, processes the discrete cosine transform coefficients extracted from the ECG signal, followed by independent component analysis to reduce the large number of features. Their method achieves 95.98% accuracy on the MIT-BIH dataset. In the time-frequency domain, wavelets have been primarily used in the literature. For instance, Can Ye at el. [8] utilizes the coefficients of discrete wavelet transform and ICA in arrhythmia classification. In addition, Assadi at el. [9] uses fractional models of a commensurate order for both normal and abnormal beats as features to a K-nearest neighbor (KNN) classifier.

To our knowledge, none of the aforementioned methods utilized the texture in ECG signal analysis in the 2D space. In this research, we propose a methodological approach that combines the benefits of other proposed approaches to automatically classify different heartbeat conditions.

Although different types of cardiovascular abnormalities can be detected from the ECG signal, we focus on detecting normal and three different abnormal heartbeat types, including the left bundle branch block, the right bundle branch block, and paced beats (see Fig. 1). Our approach is fully automated and our primary contribution is in the novel structure of the feature extraction module, where we use textural information from both the temporal and spectro-temporal domain of the ECG signal. Our method achieves a maximum accuracy of 99.81% on the MIT-BIH database, which is the most competitive one when compared to other similar approaches discussed in the literature.

The rest of the paper is organized as follows: Sections 2 and 3 discuss the methodological approach and experimental results respectively. Conclusions are discussed in Section 4.

II. METHODOLOGY

In this section, we discuss all the steps of our proposed approach as illustrated in fig. 2 above. First, for each patient, the ECG signal is preprocessed. Then, the beats extraction algorithm module follows. Next, feature extraction is performed before training and validating the classifiers used in order to

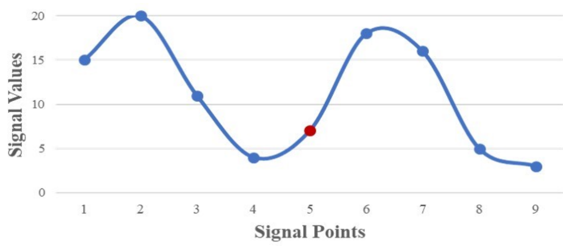

Signal values	15	20	11	4	7	18	16	5	3
Binary code	1	1	1	0		1	1	0	0
Weight	2^7	2^6	2^5	2^4		2^3	2^2	2^1	2^0
Decimal code					236				

Fig. 3 An example of 1D-LBP on a synthesis signal.

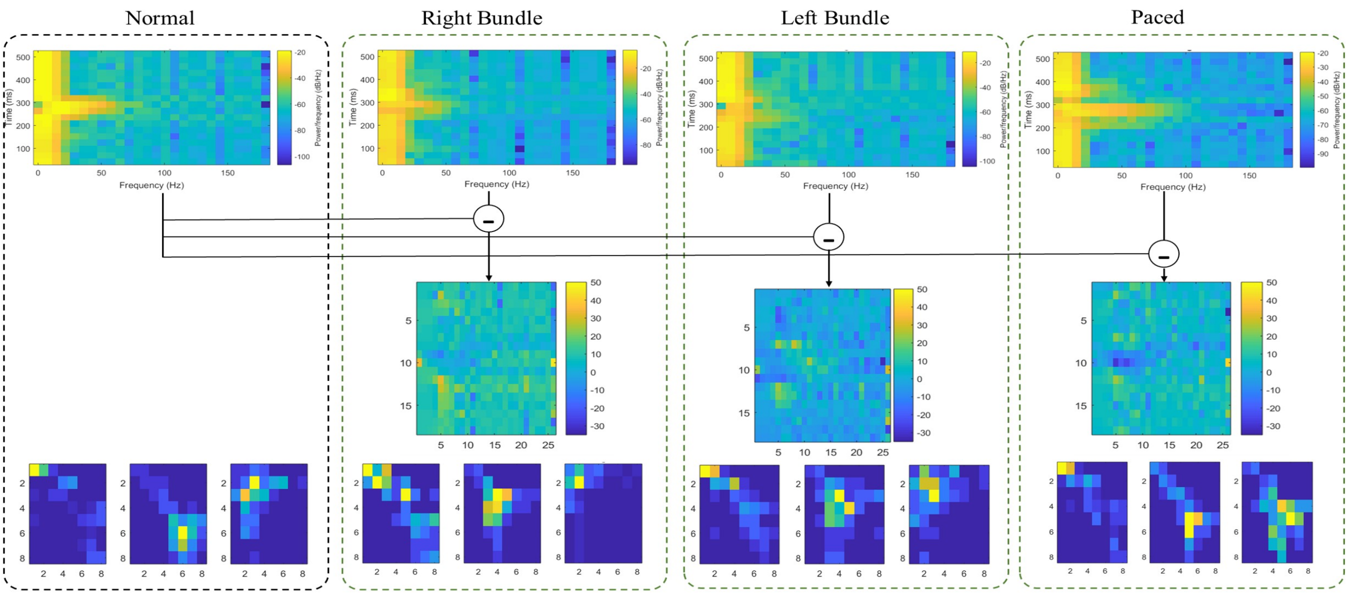

Fig. 4 The STFT images of the four beats types that reveal the difference in the frequency-time image texture. The second row shows the difference between each arrhythmia related image and the normal image. The third row is the GLCM of each of the three segments.

determine the most efficient one that classifies the heartbeat conditions (i.e. a normal and three different abnormal ones).

A. Dataset

We used the MIT-BIH arrhythmia database [10] that contains 48 patients' recordings. Each recording is two-channel, half-hour duration ECG recording that has different types of beats. The first channel, upper signal, is recorded from the modified limb lead II that is usually placed on the chest. The second channel, lower signal, is recorded from one of the modified leads V1 (V2, V4, or V5 in some recordings).

In this research, we used only four types of beats including Normal (N), Left bundle branch block (L), Right bundle branch block (R), and Paced beats (P) as shown in fig. 1. Among the four classes, the bundle branch block is an abnormal pattern that can be visually detected from the ECG. It indicates that the cardiac electrical impulse is not normally distributed across the right or left ventricles. This pattern can result in heart efficiency reduction, which can be fatal if the patient has a heart disease. Moreover, different ECG lead configurations are investigated. This includes the utilization of the first lead, the second lead, and both leads.

B. Signal Preprocessing

ECG signal processing is a challenging algorithmic module since the amplitude of the real signal, which is about 0.5 mV, is very small compared to the environment, which is 300 mV [11]. A bandpass filter is adapted to remove any frequencies other than 0.05-40 Hz. A notch filter is then used to remove the 60 Hz power line noise. Finally, signal mean normalization is performed on the signals.

C. Beats Extraction

After signal processing, we identify the QRS complexes and accordingly the heartbeats. We employ the Pan and Tompkins (P&T) [12] detector to identify the R-peaks. First, the filtered signal's derivative is estimated and squared to highlight the QRS complex. Then, windows of QRS are determined from the ECG waveform. Finally, the R peaks are detected using adaptive thresholding [12]. After the R peaks identification step, a constant number of points that account for 0.278 seconds are selected before and after each R-point having a final beat of 200 sample points and 0.556 seconds, which is sufficient enough to capture most of the heartbeat related information needed for arrhythmia classification [9].

D. Feature Extraction

Texture-based information has successfully been used before for target classification and segmentation in images [14]. The challenge here is that we have 1D signals, and thus, we can either extract the texture-based features from the time signal directly, or add to those features the frequency-related information with the expectation to increase arrhythmia classification accuracy in a follow-up step. In our time signal analysis, the 1D local binary patterns (LBP) feature extractor is used. Whereas for the time-frequency domain, the Fourier transform as well as wavelet transform are utilized to gain more information about the frequency coefficients distribution in the time signal. In addition, to take advantage of the incoming signal, we utilize the second ECG lead, since it was empirically determined that it adds more information about the beat type, which can be exploited by the selected classifier to improve its efficiency.

1) One dimensional Local binary pattern (LBP): Local binary patterns (LBP) features are conventional, yet powerful, texture descriptors that have been used widely in 2D [14]. In order to use it in the ECG signal, the 1D-LBP proposed by Chatlani et al. [15] is adapted.

The main idea is that the texture of the signal is represented with micro-patterns. Such that, signal patterns are computed by thresholding 1xP neighbors based on the value of the

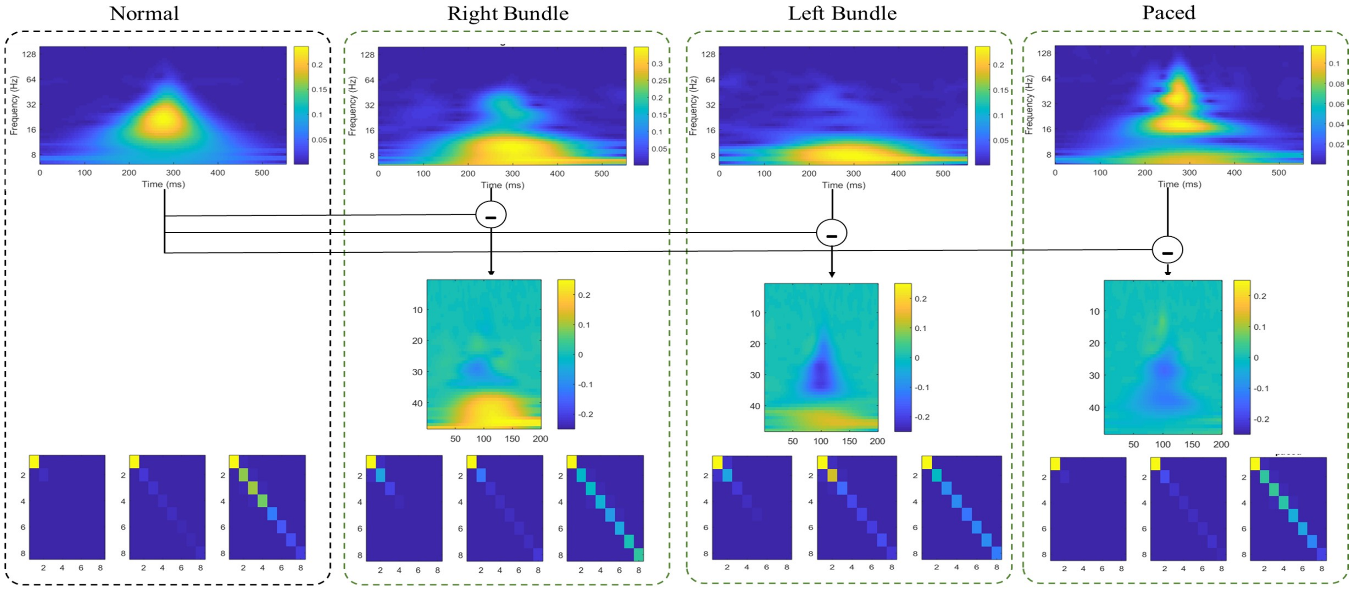

Fig. 5 The CWT images of the four beats types that reveal the difference in the frequency-time image texture. The second row shows the difference between each arrhythmia related image and the normal image. The third row is the GLCM of each of the three segments.

center point c. The resulting binary pattern is converted to a decimal value, and this is repeated for each signal point. Then a histogram is calculated for these decimal values. The equation for the LBP operator is illustrated below:

$$LBP_p(c) = \sum_{r=0}^{\frac{P}{2}-1} \Big\{ S\Big[I(c+r-\frac{P}{2}) - I(c)\Big]2^r + S\Big[I(c+r+1) - I(c)\Big]2^{r+\frac{P}{2}} \Big\} \tag{1}$$

where I is the signal intensity, and S is a sign function, that is, if the neighbor is greater than or equal to $I(c)$, then it outputs one, and zero if otherwise.

Fig. 3 shows the operation of 1D-LBP on a synthetic signal. For each signal point, the binary code is converted into decimal and then stored in its place. Next, a histogram is built for each signal which accounts for the number of incidents of each code. Therefore, for P of 8, we have 2^8, or 256, possible codes including zero. However, rotational invariant $\mathrm{LBP_r}$, an extension of LBP, neglects the rotation information in the descriptor. Further, only the "uniform" patterns are fundamental patterns of local texture [16], whereas uniform here is described as having the number of transitions less than 2 in the binary code. Uniform $\mathrm{LBP_u}$ stores all the non-uniform codes into one bin of the histogram, resulting in 2P(P-1) bins. In this paper, we adapt the rotation invariant uniform $\mathrm{LBP_{u,r}}$ that has a histogram of P+2 bins. These bins constitute for the time-domain features of our classification system.

2) Time-frequency Short-time Fourier Transform (STFT) Texture: In order to obtain more informational content from both the time and frequency domains, we utilized the STFT. Through this transformation, we can obtain the Fourier coefficients for each segment of the signal. This is controlled by a sliding window that moves through the time signal with an overlap percentage between successive windows. Thus, a time-varying spectrum can be achieved. The mathematical formula for obtaining STFT can be presented as follows:

$$STFT\{x[m]\}(n,w) = \sum_{m=-\infty}^{\infty} x[m]w[n-m]e^{jwn} \tag{2}$$

where $x[m]$ is the signal, and $w[n]$ is the sliding window. This will produce an image, in which one of the axes represents the time and the other is the frequency. Thus, more information can be gained by utilizing this representation. This is shown in the upper row of figure 4, where we can see that the left portions of the images are different. The QRS signal can be seen in the middle of the signal between 250-300 bins, and it shows the difference between the various types of beat signals. In this work, texture features of the spectro-temporal image will be used for our classification problem. The obtained image is first divided into three segments according to the frequency bandwidth. Then for each image segment, the texture features including 2D-LBP and fourteen gray level co-occurrence matrix (GLCM) Haralick features [17] including homogeneity, entropy, and contrast are computed. The bottom row of figure 4 shows the co-occurrence matrices of each beat type segment. It can be seen that each beat type exhibits different texture-based behavior, which can then be used by our classifier to distinguish them.

3) Time-frequency Wavelets Texture (CWT): One of the limitations of the Fourier transform when applied on ECG signal is that it is difficult to determine the temporal dynamics in the data. For instance, if we have a component at 30 Hz, it is difficult to say whether this component is constant over time, or just a burst of 30 Hz activity at some point in time. Thus, there is no temporal localization in the resulted Fourier transformed signal since the dot product is computed using a sine wave with constant weights overall the signal. However, wavelets provide this capability by using a weighted sine wavelet where the sine wave is multiplied by a

Gaussian function. Therefore, in this study, for the time-and/or frequency localization, we can use the continuous wavelet transform (CWT) as follows:

$$W_\psi(t,s) = \int_{-\infty}^{\infty} \frac{1}{s^n} \psi\left(\frac{\tau - t}{s}\right) x(t) d\tau \tag{3}$$

where $x(t)$ is the time signal, s is the scale, and n is the scale normalization.

In this paper, we employ the generalized Morse wavelets [18,19] which are a family of exactly analytic wavelets. The reason we utilized this wavelet family is that instead of deciding which wavelet family is better in a case-by-case analysis and asking the question of which and why one should utilize a certain wavelet family, Morse wavelets effectively merge many wavelet families. Since the ECG signals are non-stationary signals, we can use the analytic wavelets that are complex-valued time/frequency localized filters with vanishing support on negative frequencies, and whose Fourier transforms are provided only for the positive real axis. The Fourier transform of the generalized Morse wavelet is given as follows:

$$\Psi_{\beta,\gamma}(w) = \int_{-\infty}^{\infty} \psi_{\beta,\gamma}(t) e^{-i\omega t} dt = U(w) a_{\beta,\gamma} \omega^{\beta} e^{-\beta\gamma} \tag{4}$$

where $a_{\beta,\gamma}$ is a normalization constant, γ and β are the symmetry and decay parameters that controls the form of the wavelet, and $U(w)$ is the step function. The parameter γ controls the symmetry of the wavelet in time or the skewness, while β controls the duration in time. Therefore, the larger β, the broader the central portion of the wavelet and the rate of decay in time. In contrast, increasing γ broadens only the wavelet envelope. Thus, by changing the values of β and γ, the Morse wavelet can take a variety of forms. This can be used to distinguish the ECG beats since the frequency components are dissimilar. Fig 5 shows the CWT of each beat type where the aforementioned differences can be identified.

As performed with the STFT, each image is divided into three regions. Then the texture using LBP and GLCM Haralick features are extracted to represent our features. The bottom row of fig. 6 illustrates the co-occurrence matrices of each segment of the different beat types, where it can be used to discriminate our beats.

E. Classification and model validation

In the classification process, we use Support Vector Machines (SVM) [20] as well as the K-nearest neighbor (KNN) classifier for comparison. We utilize cross-validation to potentially eliminate any overfitting problems. Moreover, the performance metrics used to assess our models include the: accuracy, sensitivity, specificity, and F-score as defined below:

$$Acc_i = (TP_i + TN_i)/(TP_i + TN_i + FP_i + FN_i) \tag{5}$$

$$Sens_i = TP_i/(TP_i + FN_i) \tag{6}$$

$$Spec_i = TN_i/(TN_i + FP_i) \tag{7}$$

$$F - score_i = (2 \cdot TP_i)/(2TP_i + FP_i + FN_i) \tag{8}$$

where i is the class, and TP, TN,FP, and FN are the true positive, true negative, false positive, and false negative respectively.

III. RESULTS

We employ the texture features of the ECG signal to detect and classify four types of four heartbeats. The features are extracted using time and time-frequency domain as discussed.

Each signal is first filtered, and then normalized. The R-peaks were then detected as shown in fig. 6, where the accuracy of detection is 99% when compared to the annotation accompanied with the dataset.

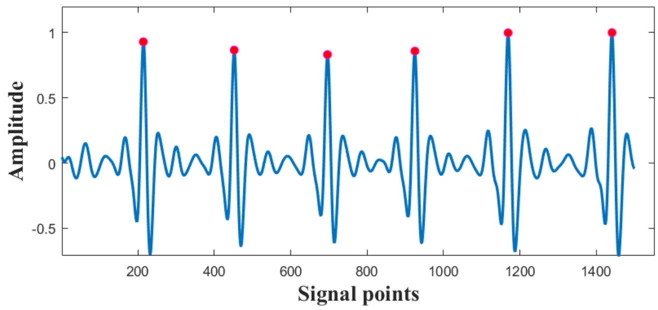

Fig. 6 R peak detection in the ECG signal of record ID = 100 in MIT-BIH dataset.

Since the data provided in the four chosen classes have a different distribution, downsampling is performed by changing the ratio involved in the training process. Table I shows the training distribution of each of the four classes where random instances were selected from each class. In addition, a 10-fold cross-validation (on both classifiers used) was performed during the training process. A kernel size of 5.7 was used for the radial basis function (RBF) SVM, while we utilized neighbors number of 5 in the KNN using Euclidean distance.

TABLE I. DISTRIBUTION OF TRAINING AND TESTING DATA CLASSES.

Beat Type	Total #	Training #	Testing #
Normal	74762	7476	67286
Left bundle block	8075	5652	2423
Right bundle block	7259	5081	2178
Paced	7028	4919	2109

The 1D-LBP was implemented, and the performance of different neighborhood size was tested. Fig. 7 shows the variation of performance measures including accuracy, sensitivity, and specificity with the P size for both SVM and KNN classifiers when we utilized the two leads of the ECG signal.

As noted, the accuracy increases with increasing the P value, which is expected since we hold more information about the signal while increasing P or the number of neighbors involved in the calculations.

A comparison of both classifiers using different configurations of ECG leads and features is illustrated in Table II. Using the LBP features, the KNN classifier over-fitted during the training, resulting in a maximum accuracy of 78.48% on the testing set using the two leads. On the other hand, the SVM resulted in a better performance than KNN, in both training and testing using the two ECG leads.

TABLE II. LBP, STFT, CWT-TEXTURE FEATURES' AVERAGE PERFORMANCE

Classifier	Perf.	LBP						STFT						CWT					
		Training			Testing			Training			Testing			Training			Testing		
		Lead V	*Lead II*	*Both leads*	*Lead V*	*Lead II*	*Both leads*	*Lead V*	*Lead II*	*Both leads*	*Lead V*	*Lead II*	*Both leads*	*Lead V*	*Lead II*	*Both leads*	*Lead V*	*Lead II*	*Both leads*
SVM	Acc.	84.89	88.96	**98.76**	79.44	82.02	**92.97**	96.93	96.57	**99.75**	96.37	95.66	**99.24**	99.01	98.99	**99.87**	98.84	98.75	**99.81**
	Sens.	86.5	88.04	98.82	82.35	82.83	91.65	98.33	99.21	99.94	97.96	98.96	99.62	98.70	98.80	99.70	98.70	96.68	98.17
	Spec.	96.9	96.44	99.66	96.63	94.47	98.38	99.79	99.92	100	99.64	99.81	99.98	99.91	99.90	99.96	99.82	99.84	99.87
KNN	Acc.	100	100	100	64.66	68.59	78.48	100	100	100	86.85	90.16	96	100	100	100	86.85	90.16	96
	Sens.	100	100	100	82.69	77.7	91.08	100	100	100	97.77	97.91	99.5	100	100	100	97.71	97.19	99.01
	Spec.	100	100	100	92.27	92.6	94.7	100	100	100	98.33	99.42	99.6	100	100	100	99.80	99.78	99.80

In the STFT, a window of size 30, and overlapping size of 20 is used to examine the frequency range of 1:180 Hz. A 2D-LBP extractor of P=8 was used for each image segment, as well as the GLCM features.

The SVM classification showed a higher performance than the KNN that achieved 96% accuracy using both leads. In addition, using only one ECG lead, an accuracy of about 96% is achieved in the SVM. Thus, independent of the texture we used, the SVM showed higher performance than KNN. In addition, the two single lead configurations showed comparable performance results. This is due to the fact that normal beats are usually distinguishable in the first lead. However, the axis for the second lead may be nearly orthogonal to the mean cardiac electrical axis. Thus, normal beats are frequently difficult to discern in the second lead while the ectopic beats will often be more prominent.

In the CWT we used β and γ values of 60 and 3 respectively, which lies between the Airy wavelet and derivative of Gaussian. A scale range of 0 to 47 was used in the detection. The same 2D-LBP extractor of P=8 was used along with the GLCM features. The accuracy of SVM (vs. KNN) was the highest in the testing set, with a training and testing accuracies of 99.87% and 99.81% respectively.

In order to analyze the cross-validation performance during the training, the boxplot of each system is plotted. Fig. 8 shows the accuracies of the ten cross-validations. The variance between the performances in each configuration is not high as shown. The figure shows that utilizing both leads always have higher accuracy than only one lead in the three approaches. On the other hand, while STFT outperforms the LBP, CWT has a better performance than both for all leads configurations.

Fig. 9 shows the performance of each beat type using the three approaches with different leads configurations. In this

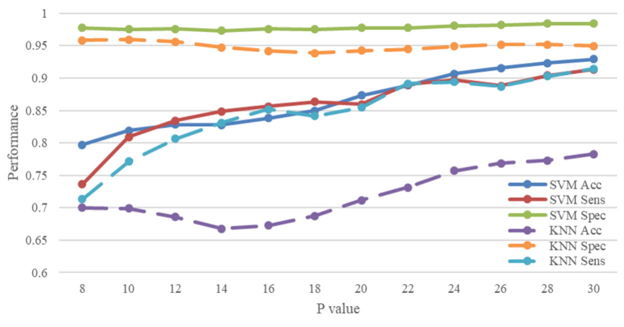

Fig. 7 Effect of P size on the testing data for both classifiers using the two ECG leads, where the SVM performance is in solid, and KNN is in dotted lines. The performance values start at 0.6

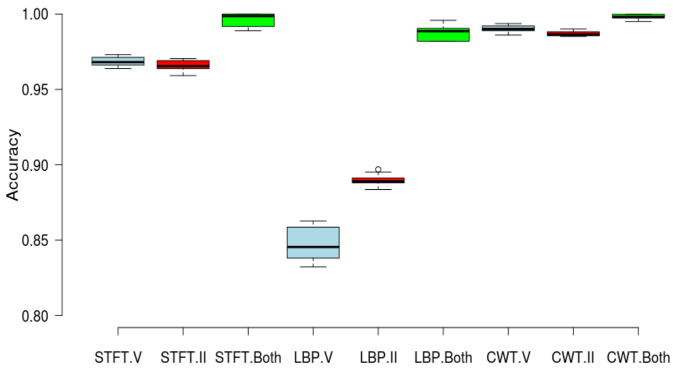

Fig. 8 Accuracy results after applying cross-validation (for all configurations used). V, II, and both are for lead V, II, and both leads respectively.

comparison, we used the F-score to get more insight into the performance since it considers both the precision and recall. Although the LBP shows high accuracy, sensitivity, and specificity measures, the F-score is low for the abnormal classes. However, the F-scores of the STFT is higher than the LBP. On the other hand, the CWT exhibits high values of all measures including the F-scores of all ECG beats.

Table III shows the comparison of our proposed system with the intra-patient approaches in the literature using MIT-BIH database. The proposed approaches outperformed other approaches discussed in the literature, as it uses all the patients including the noisy recordings and patients that had a pacemaker on. For instance, H. Tran et al [20] and N. Dewangan [4] used some selected patients instead of using the whole dataset, which can enhance the results. On the other hand, although M.Butt et al [3] used the whole 15 classes, the difference in the number of instances per class was so great that can make the grid search for the classifier parameters over-fit. For instance, the normal class has more than 70,000 instances, while some of the classes have less than 100 instances.

IV. CONCLUSION

The electrocardiogram (ECG) is one of the most common heart-monitoring tests used to detect arrhythmias. An alternative way to support automated arrhythmia detection using computer-aided tools is proposed in this paper.

Here, we investigated the classification of cardiac arrhythmia using the patient's ECG signal by assessing three types of algorithms. A temporal texture-based algorithm was utilized, which extracts the 1D-LBP features of the ECG signal. The integration of the second ECG lead (i.e. using both ECG leads configuration), has boosted the accuracy of the system

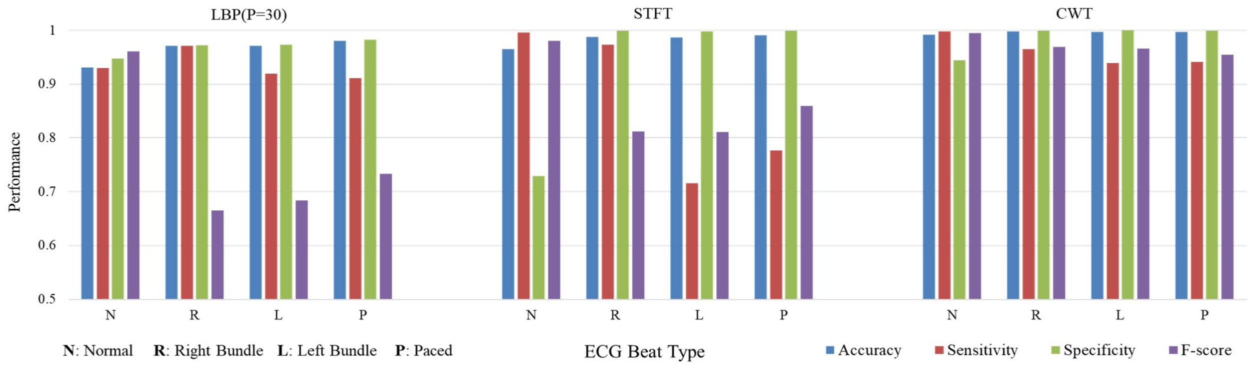

Fig. 9 Performance of each ECG beat type using different configurations, where the performance axis starts at 0.5

TABLE III. COMPARISON OF THE PROPOSED APPROACH WITH INTRA-PATIENT APPROACHES IN THE LITERATURE USING THE MIT-BIH DATABASE.

Authors	Segmentation	Features	Classifiers	Acc. %	Classes
M. Butt et al. [3]	Auto	Statistical features from temporal domain	SVM	98.78	15
N. Dewangan et al. [4]	Auto	Morphological features in temporal domain & wavelet coefficients	ANN	78.01	6
A. Charef et al. [9]	—	Frequency features	KNN	95.31	3
H. Tran et al. [21]	—	Temporal Hermite basis functions and RR-interval	Ensemble	98.63	7
Evaluated LBP	Auto	Texture in temporal domain	SVM	92.97	4
Evaluated STFT	Auto	Texture in spectro-temporal domain	SVM	99.24	4
Proposed CWT	Auto	Texture in spectro-temporal domain	SVM	99.81	4

by an average of 10%, since additional information is gained compared to the utilization of only one lead. On the other hand, spectro-temporal STFT texture features have provided more knowledge compared to only temporal information since it reflects the variation of frequency components overtime, where a boost of 7% was achieved. Nevertheless, the CWT has an overall performance improvement especially on the sub-class level with an average of 15% increase in the F-score. The SVM classifier has proven its superiority compared to KNN that suffered from over-fitting. The overall proposed system achieved an accuracy of 99.81% in the time-frequency domain using SVM classifier and an input ECG signal of 0.56 seconds. In future work, we plan to test our approach on a larger scale dataset, where more instances of the abnormal heartbeats and additional arrhythmia classes are provided.

REFERENCES

[1] Virtual Medical Center, "Arrhythmia Disease Report," 2015.

[2] R. J. Oweis and B. O. Al-Tabbaa, "QRS Detection and Heart Rate Variability Analysis: A Survey," Biomedical Science Engineering, vol. 2, no. 1, pp. 13-34, 2014.

[3] M. Butt, M. Akram, and S. Khan, "Classifying Normal Sinus Rhythm and Cardiac Arrhythmias in ECG Signals Using Statistical Features in Temporal Domain," in Asia Modelling Symposium, 2015, pp. 28-31.

[4] N. Dewangan and S. Shukla, "ECG arrhythmia classification using discrete wavelet transform and artificial neural network," in IEEE International Conference on Recent Trends in Electronics, Information & Communication Technology, 2016, pp. 1892-1896.

[5] Sung-Nien Yu and Kuan-To Chou, "Combining Independent Component Analysis and Backpropagation Neural Network for ECG Beat Classification," in International Conference of the IEEE Engineering in Medicine and Biology Society, 2006, vol. 1, pp. 3090-3093.

[6] Shing-Tai Pan, Yan-Jia Chiou, Tzung-Pei Hong, and Hung-Chin Chen, "Automatic recognition for arrhythmias with the assistance of Hidden Markov model," in International Conference on Information, Communications & Signal Processing, 2013, pp. 1-5.

[7] U. Desai, C. G. Nayak, and G. Seshikala, "An efficient technique for automated diagnosis of cardiac rhythms using electrocardiogram," in IEEE International Conference on Recent Trends in Electronics, Information & Communication Technology, 2016, pp. 5-8.

[8] Can Ye, M. Coimbra, and B.V.K. Vijaya Kumar, "Arrhythmia detection and classification using morphological and dynamic features of ECG signals," in Annual International Conference of the IEEE Engineering in Medicine and Biology, 2010, pp. 1918-1921.

[9] A. Charef, N. Belgacem, T. Bensouici, and I. Assadi, "Arrhythmias discrimination based on fractional order system and KNN classifier," in International Conference on Intelligent Signal Processing, 2015, pp. 6-12.

[10] Ary L. Goldberger, Luis Amaral, Leon Glass, Jeffrey M. Hausdorff, Plamen Ch. Ivanov, Roger G. Mark, Joseph E. Mietus, George B. Moody, Chung-Kang Peng, H. Eugene Stanley, "PhysioBank, PhysioToolkit, and PhysioNet," Circulation, vol. 101, no. 23, pp. 215-220, 2000.

[11] Ajay Bharadwaj and Umanath Kamath, "Techniques for accurate ECG signal processing," Cypress Semiconductor Corp., 2011.

[12] J. Pan and W. Tompkins, "A Real-Time QRS Detection Algorithm," IEEE Transactions on Biomedical Engineering, vol. BME-32, no. 3, pp. 230-236, 1985.

[13] H. Sedghamiz, "Matlab Implementation of Pan Tompkins ECG QRS detector," Jan. 2014.

[14] L. Nanni, A. Lumini, and S. Brahanam, "Survey on LBP based texture descriptors for image classification," Expert Syst. Appl., vol. 39, no. 3, pp. 3634-3641, 2012.

[15] N. Chatlani and J. Soraghan, "Local binary patterns for 1-D signal processing," in Signal Processing Conference, 2010.

[16] Z. Guo, L. Zhang, and D. Zhang, "Rotation invariant texture classification using LBP variance (LBPV) with global matching," Pattern Recognition, vol. 43, no. 3, pp. 706-719, 2010.

[17] R. M. Haralick, K. Shanmugam, and I. Dinstein, "Textural Features for Image Classification," IEEE Transactions on Systems, Man, and Cybernetics, vol. 3, no. 6, pp. 610-621, Nov. 1973.

[18] S.C. Olhede, and A.T. Walden, "Generalized Morse wavelets," IEEE Transactions on Signal Processing, Vol. 50, no. 11, pp. 2661-2670, 2002.

[19] Lilly, J. M., and S. C. Olhede,"Generalized Morse wavelets as a superfamily of analytic wavelets," IEEE Transactions on Signal Processing Vol. 60, no. 11, pp. 6036-6041, 2012.

[20] Hearst, Marti A., Susan T. Dumais, Edgar Osuna, John Platt, and Bernhard Scholkopf, "Support vector machines," IEEE Intelligent Systems and their applications, vol. 13, no. 4, pp. 18-28, 1998.

[21] H. L. Tran, V. N. Pham, and H. N. Vuong, "Multiple neural network integration using a binary decision tree to improve the ECG signal recognition accuracy," Int. J. Appl. Math. Comput. Sci., vol. 24, no. 3, pp. 647655, 2014.